CO adsorption and kinetics on well-characterized Pd films on Pt(111) in alkaline solutions

M. Arenz[a]*, V. Stamenkovic[b], K. Wandelt[a], P.N. Ross[b], N.M. Markovic[b]*

[a] Institut für Physikalische und Theoretische Chemie, Universität Bonn, Wegelerstr.12, D-53115 Bonn, Germany

[b] Materials Science Division, Lawrence Berkeley National Laboratory, University of California, Berkeley, CA 94720 USA

* corresponding authors: arenz@thch.uni-bonn.de, nmmarkovic@lbl.gov

Abstract

The electrochemistry of CO on a bare Pt(111) electrode as well as a Pt(111) electrode modified with pseudomorphic thin palladium films has been studied in alkaline solution by means of Fourier transform infrared (FTIR) spectroscopy. First Pd films were prepared and well characterized in UHV and subsequently transferred into the electrochemical cell for the registration of the voltammetric profiles. The charge corresponding to the formation of underpotentially deposited hydrogen (H_{upd}) on these Pt(111)-xPd surfaces was established in sulfuric acid solution as a function of x ($0 \leq x \leq 1$ Pd monolayer (ML)).

All subsequent measurements were then performed on electrochemically deposited palladium films using the above H_{upd}-charge vs. Pd coverage relationship to evaluate the amount of *electrochemically* deposited palladium. FTIR spectra for CO adsorbed on one monolayer and a submonolayer coverage are compared to those of the unmodified Pt(111) surface, all surfaces having identical 2D lattice structures. Infrared absorption bands of CO bound on either Pt(111) or Pt(111)-1ML Pd are clearly

distinguished. Spectra of CO adsorbed on Pd submonolayers show characteristic features of both CO bound to Pt and to Pd, indicating that on Pt(111)-xPd surfaces there is no coupling between Pt-CO_{ad} and Pd-CO_{ad} molecules. The kinetics of CO oxidation on these surfaces is determined either by rotating disk electrode (RDE) measurements or by FTIR spectroscopy, monitoring the CO_3^{2-} production. The oxidation of CO_{ad} on Pt(111) and on Pd modified platinum surfaces starts at the same potential, ca. at 0.2 V. The oxidation rate is, however, considerably lower on the Pt(111)-xPd surfaces than on the Pt(111) surface. The kinetics of CO oxidation appears to be determined by the nature of adsorbed hydroxyl anions (OH_{ad}), which are more strongly (less active) adsorbed on the highly oxophilic Pd atoms.

Keywords: Electrochemical methods, Reflection spectroscopy, Metal-electrolyte interfaces, Adsorption kinetics, Carbon monoxide, Platinum, Palladium

1. Introduction

The last decade has witnessed a tremendous growth in our understanding of the chemical and electronic properties of thin metal films supported on foreign metal substrates [1-9]. Only shortly after the successful UHV studies, the adsorption and catalytic properties of pseudomorphic Pd films supported on single crystal metal surfaces has also received considerable attention in the field of surface electrochemistry [10-21].

Here, we describe the preparation and characterization of Pd films evaporated on Pt(111) in ultra high vacuum (UHV) as well as the surface electrochemistry of CO on these Pt(111)-xPd surfaces in alkaline solution. In the first part of this paper we establish a correlation between UHV-prepared and -characterized Pd films and the charge corresponding to the formation of underpotentially deposited hydrogen (H_{upd}) on these Pt(111)-xPd surfaces in sulfuric acid solution. In the second part of the paper this relationship is then used for the in-situ determination of the palladium coverages which are deposited *electrochemically* on Pt(111). In order to study the electrochemistry of CO_{ad} on these Pt(111)-xPd electrodes FTIR measurements provide direct information regarding the site occupancy and interaction of CO adsorbed on Pt and Pd sites, respectively, and, thereby, the morphology of the Pd layers. Furthermore, the kinetics of CO oxidation on these surfaces is determined from FTIR measurements by monitoring the CO_3^{2-} formation. We suggest that the kinetics of CO oxidation is governed by the nature of adsorbed hydroxyl anions (OH_{ad}), which are more strongly adsorbed (and, hence, less active) on the highly oxophilic Pd atoms.

2. Experimental

2.1 UHV preparation and characterization

The Pt(111) single-crystal electrode (0.283 cm^2) used in this work was either prepared in UHV or by the well known flame annealing procedure at ambient pressure. Cleaning, characterization and Pd deposition were performed in a UHV system equipped with an angular-resolving double pass cylindrical mirror analyzer (PHI-DPCMA Φ15-255GAR) under a base pressure of $2 \cdot 10^{-10}$ torr. Sample cleaning was done by Ar^+ sputtering, annealing and removal of carbon by heating the sample in an oxygen atmosphere. This procedure was repeated until no contamination with carbon could be determined by means of Auger electron spectroscopy (AES) anymore. The Auger spectra were recorded in the derivative mode using an electron beam of 3 keV energy, 3 eV_{p-p} modulation and 5 μA beam current, in a range from 140 to 900 eV. Different amounts of palladium were deposited onto the clean Pt(111) surface using a UHV evaporator Omicron/Focus model EFM3/4, equipped with an integrated flux monitor. The deposition of Pd was followed by simultaneously recording the AES signal for Pt at 64 eV in a range of ±10eV. After deposition the total coverage of Pd was also determined by low energy ion scattering (LEIS). The LEIS spectra were recorded using a He^+ ion beam with an energy of 1 keV and a sample current between 5 to 100 nA, in order to minimize the sputtering effects by the ion beam. The incidence angle was 45° and the scattering angle was 127°. The ion beam was rastered over an area of 3×3 mm^2 and the time of recording one spectrum was 60 s.

2.2 Electrochemical measurements

The pretreatment and mounting of the Pt(111) single crystal in a rotating disc electrode (RDE) configuration was fully described previously [22]. In short, following crystal cleaning either by flame annealing or UHV treatment described above, the crystal

was protected by a drop of ultra pure water in an argon stream, transferred to and mounted into the disk position of an insertable disk electrode assembly (*Pine Instruments*). Subsequently the electrode was transferred into the electrochemical cell. For the electrochemical deposition of palladium the clean, flame annealed sample was subjected to a potential cycling between $0.05 < E < 0.9$ V in a 0.05 M H_2SO_4 + $5 \cdot 10^{-6}$ M Pd^{2+} solution with a sweep rate of 50 mV/s. The amount of Pd deposited was controlled by monitoring the continuous change of the voltammetric features from those characteristic of bare Pt(111) to those of a pseudomorphic monolayer of palladium (see for example ref. 23). Afterwards the electrode was rinsed with ultra pure water and transferred either into the *in-situ* FTIR cell or to a standard three compartment electrochemical cell for kinetic measurements, both containing 0.1 M KOH.

Sulfuric acid and potassium hydroxide solutions were prepared from concentrated sulfuric acid (*Baker Ultrex*) and KOH pellets (*Aldrich Semiconductor Grade*), respectively, using triply pyrodistilled water. Prior to each experiment all solutions were deaerated by purging with argon (Air Products 5N5 purity). The CO (Spectra Gases N4.5) measurements were carried out in CO saturated electrolytes. Before each measurement the electrode was held at 0.05 V for 3 min. in order to obtain a fully CO covered surface. The RDE CO oxidation measurements were performed under a continuous flux of CO dissolved in the (bulk) electrolyte (CO_b). The reference electrode for the electrochemical cells was a saturated calomel electrode (SCE) separated from the working electrode compartment by a closed electrolyte bridge in order to avoid chloride contamination. All potentials shown in the text, however, refer to the reversible hydrogen

electrode in the same solution, calibrated from the reversible potential for the hydrogen evolution/oxidation reaction.

2.3 FTIR measurements

For the in situ FTIR measurements a Nicolet Nexus 670 spectrometer was available with a nitrogen cooled MCT detector. All IR measurements were performed in a spectroelectrochemical glass cell designed for an external reflection mode in a thin layer configuration. The cell is coupled at its bottom with a CaF_2 prism beveled at 60° from the surface normal. Prior to each measurement a cyclic voltammogram was recorded in order to check the cleanliness of the electrode surface. Subsequently the solution was saturated with CO for at least 3 min. holding the electrode potential at 0.05 V. The spectra were recorded with a resolution of 8 cm^{-1}. All measurements were performed using p-polarized light. In order to obtain a single beam spectrum 50 scans were collected at each potential resulting in a recording time of 25 s. Absorbance spectra were calculated as the ratio $-\log(R/R_0)$ where R and R_0 are the reflectance values corresponding to the sample and reference spectra, respectively. Reference spectra were recorded either at 0.9 V or –0.05 V, where CO_{ad} is completely oxidized and before the onset of CO_{ad} oxidation, respectively. The reference potential in the spectroelectrochemical cell was controlled by a reversible hydrogen electrode (RHE).

3. Results and Discussion

3.1 LEIS-CV characterization of Pt(111)-Pd surfaces

The surface coverages of the UHV-prepared Pd films on Pt(111) are obtained by the use of LEIS, see Figure 1. The spectrum for unmodified Pt(111) with the ratio of the

energy of incident and scattered He^+ ions (E_1/E_0) of 0.94 is clearly resolved in Figure 1e) (dashed line). Deposition of Pd leads to a gradual decrease in the Pt peak and an increase of the LEIS peak with a ratio of $E_1/E_0 = 0.89$, indicating that the latter peak corresponds to He^+ ions scattered from palladium surface atoms. Since the elemental sensitivity factors for palladium and platinum are about the same, the Pd/Pt ratio and, thus, the Pd coverage can simply be calculated by fitting the area of both peaks using Gaussian lines. LEIS spectra of representative examples for Pd surface coverages in the range of $40\% < \Theta_{Pd} < 80\%$ are shown in Figure 1b-d. In Figure 1e only a single peak of $E_1/E_0 = 0.89$ with the maximum intensity is resolved in the LEIS spectrum (solid line). Therefore the Pt surface is completely covered by Pd atoms, which is in agreement with previous AES/LEED studies by Attard and co-workers [10, 13].

In order to establish the relationship between the palladium surface coverage as determined with LEIS and the corresponding voltammetric profile the respective Pt(111)-xPd sample was immediately transferred to the electrochemical cell. Considering that the voltammetric response of the Pt(111) electrode modified with a Pd film is well established in sulfuric acid solution [11, 12, 16, 23], in this work the UHV-prepared Pt(111)-xPd systems were electrochemically characterized in 0.05 M H_2SO_4 at room temperature, as shown in Figure 1a. For comparison the CV of pure Pt(111) is included as well. Clearly, an increase in the surface coverage of Pd leads to a concomitant increase in the height of the CV-peak at 0.23 V, reaching the maximum for the Pt(111)-xPd surface shown in Figure 1e. Notice, however, that the peak associated with the formation of the second Pd layer (at ca. 0.28 V [12]) is not observed in the cyclic voltammogram, suggesting that less than or equal to 1 ML is evaporated on the Pt(111) surface. In turn,

from the fact that no Pt-peak has been observed in the LEIS spectrum (Figure 1e), we conclude that indeed just 1ML is deposited on the surface. With increasing the Pd coverage the observed current density in the potential region of sulfate desorption/adsorption (0.375 V < E < 0.55 V) on Pt(111) decreases. For the Pt(111)-1MLPd surface the processes of hydrogen adsorption/desorption and bisulfate desorption/adsorption (0.05 V < E < 0.375 V) exhibit a single very sharp peak centered at ca. 0.23 V, as observed previously on an electrochemically prepared Pd monolayer [16, 17, 23]. A further analysis of the cyclic voltammograms in Figure 1 revealed that the hydrogen adsorption pseudocapacitance increases from 160 $\mu C/cm^2$ on unmodified Pt(111) to 320 $\mu C/cm^2$ on Pt(111) covered with 1 ML of Pd [16]. The difference between the total charge in the H_{upd} potential region (Q_{Hupd}) and the charge deduced from bisulfate adsorption (80 $\mu C/cm^2$) equals 240 $\mu C/cm^2$, implying that the Pt(111)-1ML Pd surface is covered by 1 ML of H_{upd} [16]. The relationship between Θ_{Pd}, evaluated from the LEIS measurements, and Q_{Hupd}, inferred from the corresponding cyclic voltammograms, is shown in Figure 2. Clearly, the integrated charge increases linearly from a value of 166 $\mu C/cm^2$ (Θ_{Pd} = 0 ML) to a charge of 320 $\mu C/cm^2$ (Θ_{Pd} = 1 ML). This calibration curve can now be used to evaluate *in-situ* and *quantitatively* the surface coverage of palladium deposited *electrochemically* on Pt(111). The surface coverage of palladium is determined from Figure 2, simply by integrating the charge in the H_{upd} region (0.05 V < E < 0.375 V) on the respective Pt(111)-xPd electrode and reading the corresponding Θ_{Pd} value off the calibration diagram.

3.1 Surface chemistry of CO on Pt(111)-xPd electrodes: FTIR measurements

In this section, in situ studies of CO adsorption and the kinetic behavior of CO oxidation on the Pt(111)-xPd surfaces are presented. Using FTIR spectroscopy, the surface chemistry of CO in alkaline solution is correlated with the surface coverage of Pd *electrochemically* deposited on a Pt(111) electrode. Alkaline rather then acid solution is used, because the electrocatalysis of CO on Pt(111) in alkaline solution shows an exceptionally high activity, e.g., the onset of CO oxidation is observed deep in the H_{upd} potential region.

The voltammetric behavior of a Pt(111)-1MLPd electrode at 298 K in 0.1 M KOH solution is shown in Figure 3a (solid curve). For comparison, the voltammogram of a bare Pt(111) electrode, obtained under the same experimental conditions, is also included (dashed curve). It can be seen that the voltammogram of bare Pt(111) exhibits three separate potential regions: the hydrogen underpotential deposition region (H_{upd}, $0 < E < 0.4$ V) is directly followed by the double layer potential region (ca. $0.4 \text{ V} < E < 0.6$ V) and subsequently by the so-called 'butterfly region' ($0.6 < E < 0.9$ V), which is commonly assumed to represent the discharge of OH^- to form a hydroxyl adlayer [24], hereafter denoted as OH_{ad}. At more positive potentials the "irreversible" oxide formation is observed at $E > 0.8$ V. Notice that, very recently, it was demonstrated that on Pt(111) in alkaline electrolyte some amount of OH_{ad} can even be present in the H_{upd} region [31]. Based on thermodynamic considerations, it was estimated that the Pt-OH_{ad} bond energy in the H_{upd} potential region is in the range of ca. 206-216 kJ/mol. This is considerably higher than the estimated Pt-OH bond energy in the "butterfly region", which is ca 136 kJ/mol.

When a monolayer of Pd is deposited on Pt(111), the voltammogram changes dramatically. In particular, the formation of 1ML of H_{upd} ($0.05 < E < 0.34$ V) is *immediately* followed first by the reversible adsorption of OH_{ad} (a relatively sharp reversible peak at 0.475 V), and then by the "true oxide formation". A further inspection of the cyclic voltammogram reveals that the OH^- adsorption on the Pt(111)-1MLPd surface, as for bare Pt(111), may even start in the H_{upd} potential region. Nevertheless, regardless of the true incipient potential for the OH^- adsorption on the Pd surface, Figure 3a clearly shows that in comparison to the Pt(111)-OH_{ad} interaction, the reversible adsorption of OH^- on the Pd covered surface is shifted towards more negative potentials. This confirms previous findings that the Pd-OH_{ad} bond is stronger than the Pt-OH_{ad} bond, e.g. Pd is a more oxophilic metal than Pt [9]. As we demonstrate below, the differences in the bond energy between Pt-OH_{ad} and Pd-OH_{ad} will have a significant effect on the electrocatalysis of CO on the Pt(111)-xPd surfaces.

The characteristic C-O stretching bands for bare Pt(111) in CO saturated 0.1 M KOH solution as a function of the electrode potential are shown in Figure 4a. The background spectra are collected at 0.9 V, where CO_{ad} is completely oxidized. As previously described by different authors [25-28], at potentials below 0.3 V characteristic C-O stretching bands near 2070 cm^{-1} and 1740 cm^{-1} predominate in the spectra. These bands can be assigned to CO bound on a-top and three fold hollow sites, respectively. Going to more anodic potentials, the band of the hollow species is replaced by a new C-O stretching band at about 1800 cm^{-1}, which can be related to the presence of bridge bonded CO. Comparison of the potential dependent intensity changes for the three-fold and bridge CO bands with surface X-ray scattering (SXS) data suggested that the three-fold

hollow band is related to a p(2 x 2)-3CO structure whereas the loss of this ordered structure is reflected by the appearance of the bridge-bonded CO band [29]. This change in the adsorption geometry is accompanied by the onset of CO oxidation (CO_3^{2-} production in Figure 5c), which begins at a potential as low as 0.2 V. As discussed in reference [30], CO_{ad} is oxidatively removed in the H_{upd} potential region by OH_{ad} which is adsorbed at the defect/step sites of the Pt(111) surface. More details about the structure stability of a CO_{ad} layer and the kinetics of CO oxidation the interested reader may find in reference [30, 31].

For Pt(111) covered with a full monolayer of Pd FTIR spectra in CO saturated 0.1 M KOH (Figure 4b) reveal only one single absorption band near 1870 cm^{-1}. Previous FTIR investigations of CO adsorption on Pd in acid solutions also showed only one absorption band at about 1900 cm^{-1}. The absorption peak in acid solutions was assigned to bridge bonded CO_{ad} [23, 32]. In line with this study, the band for CO on 1 ML of Pd in alkaline solution also may be assigned as CO_{ad} at bridge sites. Note that the observation of the C-O stretching bands at lower wave numbers than in acid solutions (ca 30 cm^{-1}) may be related to the lower surface potential in alkaline solution, as previously discussed for the Pt(111)-CO_{ad} system [33]. A closer inspection of Figure 4b reveals that besides the major Pd-CO band also a tiny band at about 2020 cm^{-1} is present in the spectra. From Figure 4a it is clear that this band corresponds to adsorption of CO on very *small* Pd-free platinum islands. Therefore, we conclude that if only a single band near 1870 cm^{-1} is observed in the spectra, the Pt(111) electrode is covered with a pseudomorphic palladium monolayer. The pseudomorphic growth of palladium on Pt(111) and its stability in acid [18] and alkaline solutions is confirmed by SXS measurements. Figure 5b also shows that

sweeping the potential from –0.05 V to more positive values, the integrated intensities for CO_{ad} on Pt(111)-1MLPd remain constant, suggesting that the initial slow oxidation of CO (production of CO_3^{2-} in Figure 5c) is accompanied by concomitant re-adsorption of CO from the CO saturated solution in the thin layer. Note that with increasing the potential the absorption band is becoming broader, indicated by the change of the full width of half maximum (FWHM) from 20 cm^{-1} at 0 V to 31.5 cm^{-1} at 0.4 V. Above 0.4 V, however, the decrease in the integrated intensity of CO (Figure 5b) parallels a fast oxidation of CO at these high anodic potentials. Note also, that due to an interplay of the electrochemical Stark effect [34] and dipole-dipole coupling the absorption frequency of CO is dependent on the electrode potential [28].

Another point that can be clarified from the in-situ FTIR measurements is, that although the onset of CO_3^{2-} production associated with the CO oxidation on Pt(111) and Pt(111)-1MLPd surfaces is very similar (close to 0.2 V), the rate of CO_3^{2-} produced on Pt is higher than on Pt(111)-1MLPd. A comparison (Figure 5b) clearly shows that despite the same onset potential of CO oxidation the absorption bands of CO on Pt(111)-1MLPd can still be observed at potentials as high as 0.7 V. This suggests that the rate of CO oxidation, which proceed according to the Langmuir-Hinshelwood reaction mechanism, e.g.,

$$CO_{ad} + OH_{ad} + OH^- \xrightarrow{K_{ox}} CO_2 + e^- + H_2O \qquad (1)$$

is much faster on Pt(111) than on a Pt(111)-1MLPd electrode. This is confirmed by RDE results summarized in Figure 3b for the oxidation of CO_b on Pt(111) and Pt(111)-1MLPd electrodes at ambient temperature. It is obvious that the overall reaction rate of CO_b oxidation is much faster on Pt(111) than on the palladium modified electrode. Note that

the apparent difference in the onset potential compared to the potentiostatic FTIR measurements can be explained by the relatively high scanning rate of 50 mV/s.

This might be surprising results considering that the adsorption of OH_{ad} is enhanced on Pt(111)-1MLPd, see Figure 3a. To resolve this paradox one should recall that the kinetics of reaction (1) does not only depend on the surface coverage of OH_{ad}, but is also strongly affected by the delicate balance between the *coverage and the nature* of the electroactive species. That is, as in the electrochemical kinetics of inorganic/organic compounds, the CO oxidation is governed by the same electrocatalytic law: while the reaction rate passes through a maximum for metals adsorbing CO and OH^- moderately strong, the kinetic rates are very slow on those metals which adsorb CO and OH^- either strongly or weakly. Our previous studies have shown that while the energetics of CO adsorption are not significantly different on Pt(111)-1MLPd from the one found for Pt(111)-CO_{ad}, the adsorption of anions on Pd is much stronger than on Pt. Consequently, the Pd-OH_{ad} bond is much stronger than the Pt-OH_{ad} bond. We propose that, because the Pd-OH_{ad} bond is very strong (especially at more anodic potentials), the catalytic activity of OH_{ad} towards the oxidation of CO_{ad} is significantly reduced on Pt(111)-1MLPd in comparison with OH_{ad} which is adsorbed on Pt(111). A more detailed description of catalytic properties of thin palladium films supported on Pt(111) will be given elsewhere [35].

For the characterization of the adsorption behavior of CO on Pt(111)-xML Pd electrodes further FTIR spectroscopic measurements were performed. Even though FTIR spectra were recorded on six different samples, only one surface with $\Theta_{Pd} = 0.43$ ML, shown in Figure 4c, will here be introduced as an example to demonstrate all important features of CO surface electrochemistry on a Pd modified Pt(111) surface in the Θ_{Pd}

submonolayer range in alkaline solution. Figure 4c shows a set of absorption spectra for adsorbed CO on Pt(111)-0.43MLPd in CO saturated 0.1 M KOH. At low potentials, three different C-O stretching bands near 1730 cm^{-1}, 1870 cm^{-1} and 2035 cm^{-1} can be distinguished in the spectra. By comparison with Figures 4a and 4b, these bands can clearly be assigned to multi coordinated CO adsorbed on Pt, CO bridge bonded on Pd and on-top CO adsorbed on Pt, respectively. Figure 5c shows that the oxidation of CO, as on the previous two surfaces, begins at around 0.2 V, concurrent with the loss of Pt-CO_{ad} at three fold hollow sites and the emergence of Pt-CO_{ad} on bridge sites. At more positive potentials, further CO_3^{2-} production (Figure 5c) is accompanied by the loss of Pt-CO_{ad} and Pd-CO_{ad} at the bridge sites and Pt-CO_{ad} at atop sites, see Figure 5a and b. As for the Pt(111)-Ru-CO system studied by Stimming and co-workers [36], this result reveals that no coupling between Pt-CO_{ad} and Pd-CO_{ad} molecules takes place on the Pt(111)-xPd surfaces. Furthermore, this result suggests that Pd appears to be deposited on Pt(111) in metallic islands (or patches) [36], as was previously established by Clavilier et al. from voltammetric measurements [12]. Thus, in-situ FTIR experiments performed with CO may serve as an indirect probe for the determination of the Pd morphology on the Pt(111) substrate. Finally, we emphasize that the kinetics of CO oxidation on Pt(111)-0.43MLPd, established from the onset/slope of CO_3^{2-} production in Figure 4c, lies between the one observed of pure Pt(111) and Pt(111) modified by 1ML of Pd. In fact, as we will demonstrate in a forthcoming paper, a monotonic increase in the palladium surface coverage leads to a gradual decrease in the catalytic activity of the Pt(111)-xPd surfaces. This implies that the catalysis of CO on these surfaces takes place *independently* on Pt

and Pd sites, i.e. in contrast to Pt-Pd(hkl) single crystal surfaces [37] the Pt(111)-xPd systems do not behave as a pseudo metal.

4. Conclusion

The CO adsorption behavior and the kinetics of CO oxidation on bare Pt(111) and Pt(111)-xPd electrodes in 0.1 M KOH has been studied by means of Fourier transform infrared (FTIR) spectroscopy. Pd films are prepared and characterized in UHV utilizing ex-situ probes such as Auger electron spectroscopy and low energy ion scattering techniques. These well characterized surfaces are transferred into an electrochemical cell for the analysis of the voltammetric profiles of Pt(111)-xPd surfaces. The correlation between the Pd coverage of UHV-characterized Pd films and the charge corresponding to the formation of underpotentially deposited hydrogen (H_{upd}) is used in further experiments to evaluate in-situ the amount of palladium which is deposited *electrochemically* on Pt(111). FTIR measurements were performed on such *well characterized, electrochemically* deposited Pd films. The spectra for CO adsorbed on a pseudomorphic monolayer of Pd and a Pd submonolayer, with a Pd coverage of about 40 % Pd, are compared to those of the unmodified Pt(111) surface, all surfaces having identical 2D lattice structures. Infrared absorption bands of CO bound on bare Pt(111) and Pt(111)-1MLPd can clearly be distinguished. Spectra of CO adsorbed on the Pd submonolayer reveal both the characteristic features of CO bound on Pt and CO bound on Pd, indicating that there is no coupling between Pt-CO_{ad} and Pd-CO_{ad} molecules on Pt(111)-xPd surfaces. These results indicate that Pd is deposited on Pt(111) in the form of metallic islands. The kinetics of CO oxidation on these surfaces was determined by monitoring the CO_3^{2-} production during oxidative removal of CO_{ad} from Pd-free and

Pd-modified Pt(111). The oxidation of CO_{ad} on Pt(111) and on platinum modified surfaces with Pd starts at the same potential, ca. at 0.2 V. The oxidation rate, however, is considerably lower on Pd-modified Pt(111) than on bare Pt(111). It is proposed that the kinetics of CO oxidation is determined by the nature of the adsorbed hydroxyl anions (OH_{ad}), which are much stronger adsorbed (less active) on the highly oxophilic Pd layers.

References

[1] Rodriguez, J.A.; Goodman, D.W.; Science **257** (1992) 897

[2] Campbell, R.A.; Rodriguez, J.A.; Goodman, D.W.; Phys. Rev. B. **46** (1992) 7077

[3] Han, M.; Mrozek, P.; Wieckowski, A. Phys. Rev. B. **48** (1993) 8329

[4] Sellidj, A.; Koel, B.E.; Surf. Sci. **284** (1993) 139

[5] Sellidj, A.; Koel, B.E.; Phys. Rev. B. **49** (1994) 8367

[6] Poulston, S.; Tikhov, M.; Catal. Lett. **42** (1996) 167

[7] Hammer, B.; Morikawa, Y.; Norskow, J.K.; Phys. Rev. Lett. **76** (1996) 2141

[8] Mavrikakis, M.; Hammer, B.; Norskow, J.K.; Phys. Rev. Lett. **82** (1998) 2819

[9] Pallassane, V.; Neurock, M.; Hansen, L.; Hammer, B.; Norskow, J.K.; Phys. Rev. B **60** (1999) 6141

[10] Attard, G.A.; Bannister, A.; J. Electroanal. Chem. **300** (1991) 467

[11] Clavilier, J.; Llorca, M.J.; Feliu, J.M.; Aldaz, A.; J. Electroanal. Chem. **310** (1991) 429

[12] Llorca, M.J.; Feliu, J.M.; Aldaz, A.; Clavilier, J.; J. Electroanal. Chem. **351** (1993) 299

[13] Attard, G.A.; Price, R.; Al-Akl., A.; Electrochim. Acta **39** (1994) 1525

[14] Baldauf, M.; Kolb, D.M.; Electrochim. Acta **38** (1993) 2145

[15] Baldauf, M.; Kolb, D.M.; J. Phys. Chem. B **100** (1996) 11375

[16] Climent, V. ; Markovic, N.M.; Ross, P.N.; J. Phys. Chem. B **104** (2000) 3116

[17] Alvarez, B. ; Climent, V. ; Rodes, A. ; Feliu, J.M. ; J. Electr. Chem. **497** (2001) 125

[18] Markovic, N.M.; Lucas, C.; Climent, V.; Stamenkovic, V.; Ross, P.N.; Surf. Sci. **465** (2000) 103

[19] Kibler, L.A.; Kleinert, M.; Randler, R.; Kolb, D.M.; Surf. Sci. **443** (1999) 19

[20] Naohara, H.; Ye , S.; Uosaki, K.; J. Phys. Chem. B **102** (1998) 4366

[21] Naohara, H.; Ye , S.; Uosaki, K.; Colloids Surf. A **154** (1999) 201

[22] Markovic, N.M.; Gasteiger, H.A.; Ross, P.N.; J. Phys. Chem. **99** (1995) 3411

[23] Gil, A.; Clotet, A.; Ricart, J.M.; Illas, F.; Alvarez, B; Rodes, A.; Feliu, J.M.; J. Phys. Chem. B **105** (30) (2001) 7263-7271

[24] Wagner, F.T.; Ross, P.N.; J. Electroanal. Chem. **250** (1988) 301

[25] Kitamura, F.; Takahashi, M.; Ito, M.; Surf. Sci. **223** (1989) 493

[26] Chang, S.C.; Weaver, M.J.; Surf. Sci. **238** (1990) 42

[27] Rodes, A.; Gomez, R.; Feliu, J.M.; Weaver, M.J.; Langmuir **16** (2001) 811

[28] Akeman, W; Friedrich, K.A.; Stimming, U.; J. Chem. Phys. **113** (2000) 6864

[29] Lucas, C.; Markovic, N.M; Ross, P.N.; Surf. Sci. **425** (1999) L382

[30] Schmidt, T.J.; Ross, P.N.; Markovic, N.M.; accepted for publication in J. Phys. Chem. B

[31] Markovic, N.M.; Grugur, B.N.; Lucas, C.; Ross, P.N.; J. Phys. Chem. B **103** (1999) 497

[32] Zou, S.; Gomez, R.; Weaver; J. Electroanal. Chem. **474** (1999) 155

[33] Wasileski, S.A.; Koper, M.T.M.; Weaver, M.J.; J. Phys. Chem. B **105** (2001) 3518

[34] Nichols, R.J.; in "*Adsorption of Molecules at Metal Electrodes*", ed. by J. Lipkowski and P.N. Ross, VCH Wiley 1992

[35] Arenz, M;, Wandelt, K; Stamenkovic, V.; Schmidt, T.J.; Markovic, Ross, P.N.; in preparation

[36] Friedrich, K.A.; Geyzers, K.-P.; Linke, U.; Stimming, U.; Stumper, J.; J. Electroanal. Chem. **402** (1996) 123

[37] Schmidt, T.J. et al. in preparation

Figure Captions

Figure 1: a) Cyclic voltammetry for Pt(111)-xPd recorded in 0.05 M H_2SO_4 (sweep rate 50 mV/s) with various amounts of palladium deposited in UHV at room temperature; b-e) corresponding LEIS spectra after palladium deposition; He^+ energy = 1 keV ; Pd coverage calculated by fitting two Gaussian lines; in 1e) the LEIS spectrum of bare Pt(111) is included as a reference (dashed line)

Figure 2: Calibration curve of the integrated H_{upd} charge (between 0.05 and 0.375 V (RHE)) in the voltammograms from UHV deposited Pd films versus the Pd coverage evaluated by LEIS

Figure 3: a) Cyclic voltammetry of Pt(111)-1ML (full line) and Pt(111) (dashed line) recorded in 0.1 M KOH (sweep rate 50 mV/s) at room temperature; b) RDE CO_b electrooxidation on Pt(111)-1ML and Pt(111) in 0.1 M KOH at room temperature; 50 mV/s, rotation rate 2500 rpm

Figure 4: Series of infrared spectra of CO_{ad} on (a) Pt(111), (b) Pt(111)-1MLPd and (c) Pt(111)-43%Pd obtained by stepping the applied potential in a positive direction in CO sat. 0.1 M KOH solution, each spectrum was accumulated from 50 interferometer scans at the potential indicated, the background potential was taken at 0.9 V vs. RHE;

Figure 5: Integrated band intensities of on-top Pt-CO bands (a) and Pd-CO bands (b) as a function of the electrode potential c) CO_3^{2-} production for all three surfaces as a function of the electrode potential, data extracted by using –0.05 V as background potential

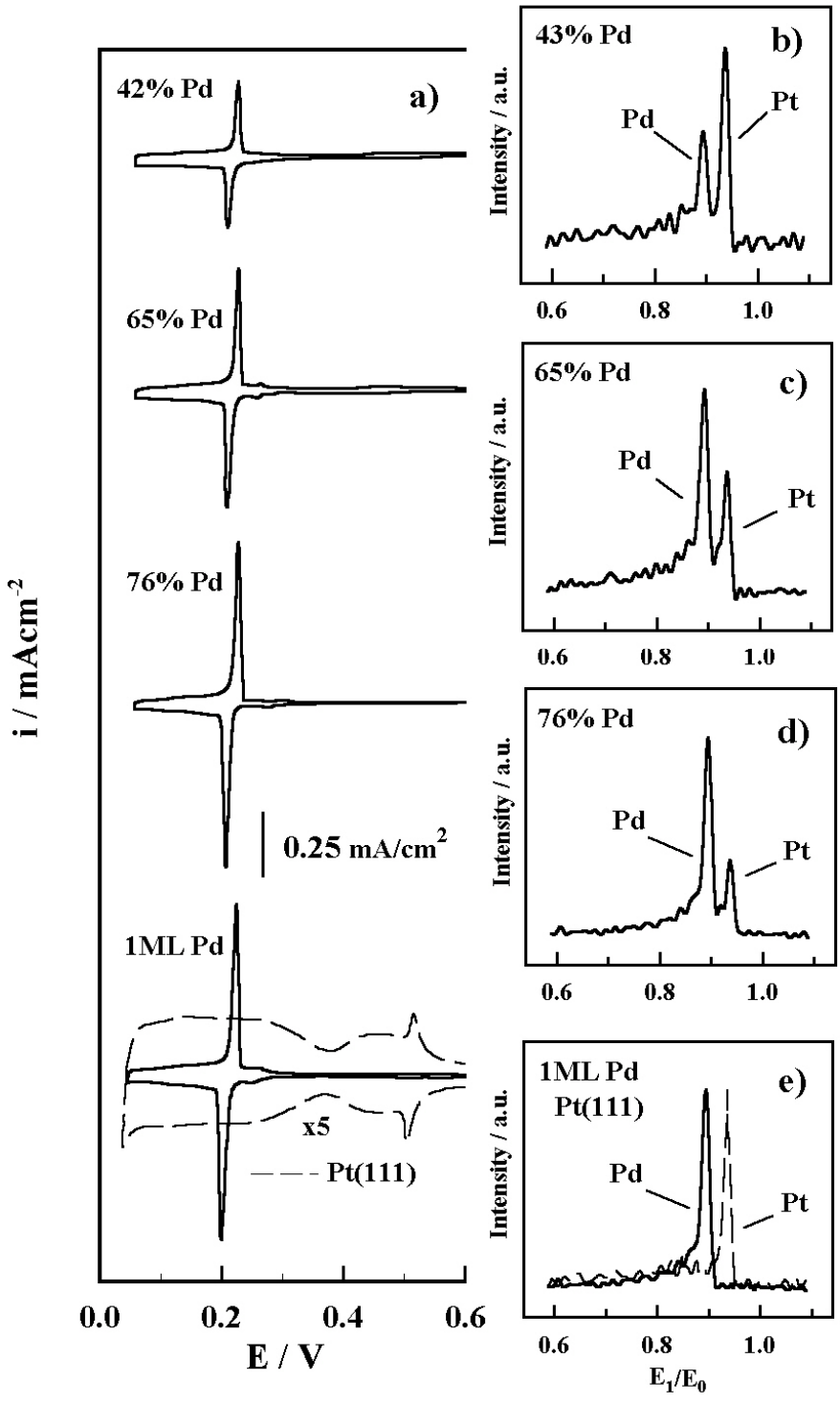

Arenz et al. figure 1

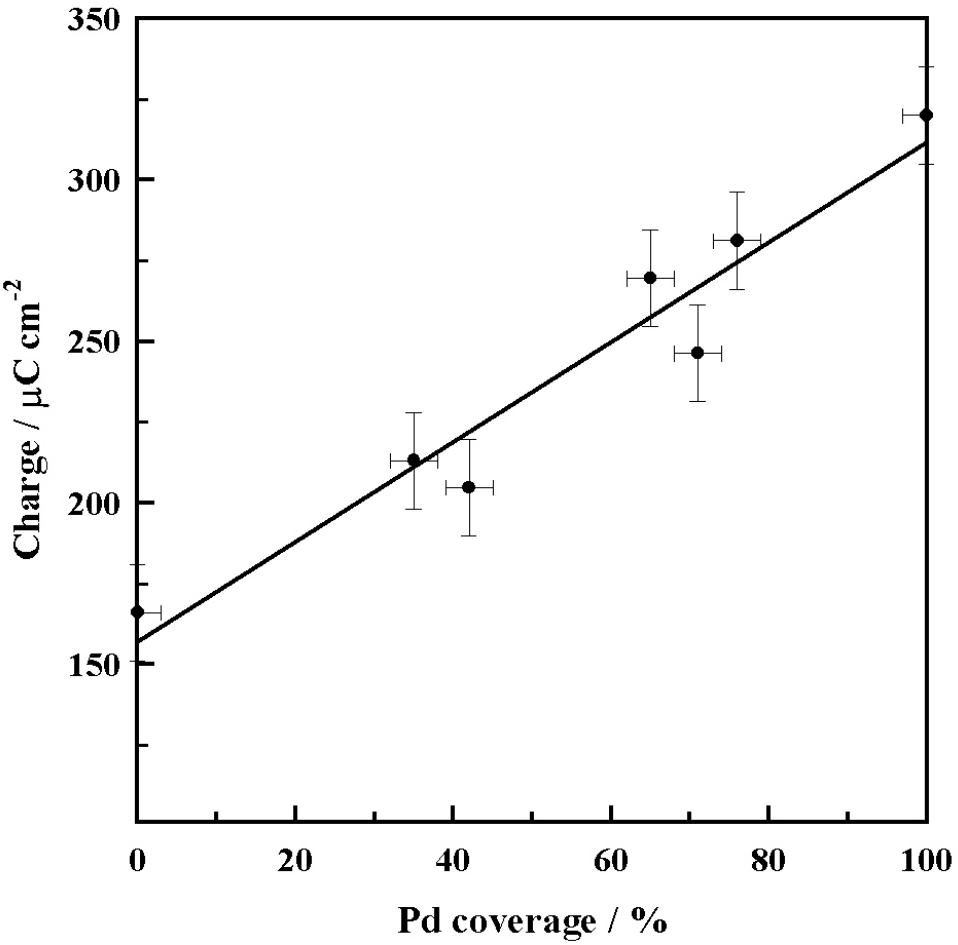

Arenz et al. figure 2

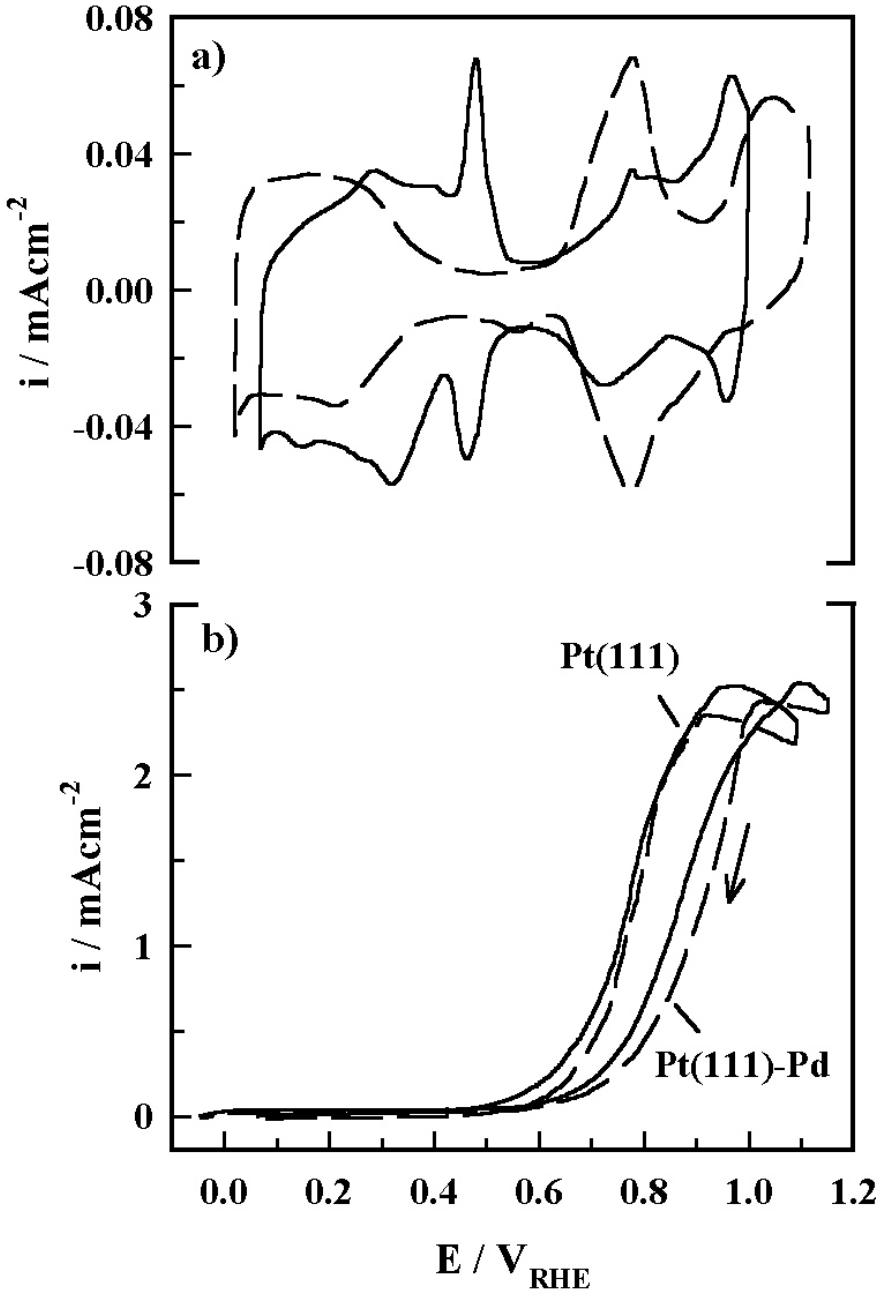

Arenz et al. figure 3

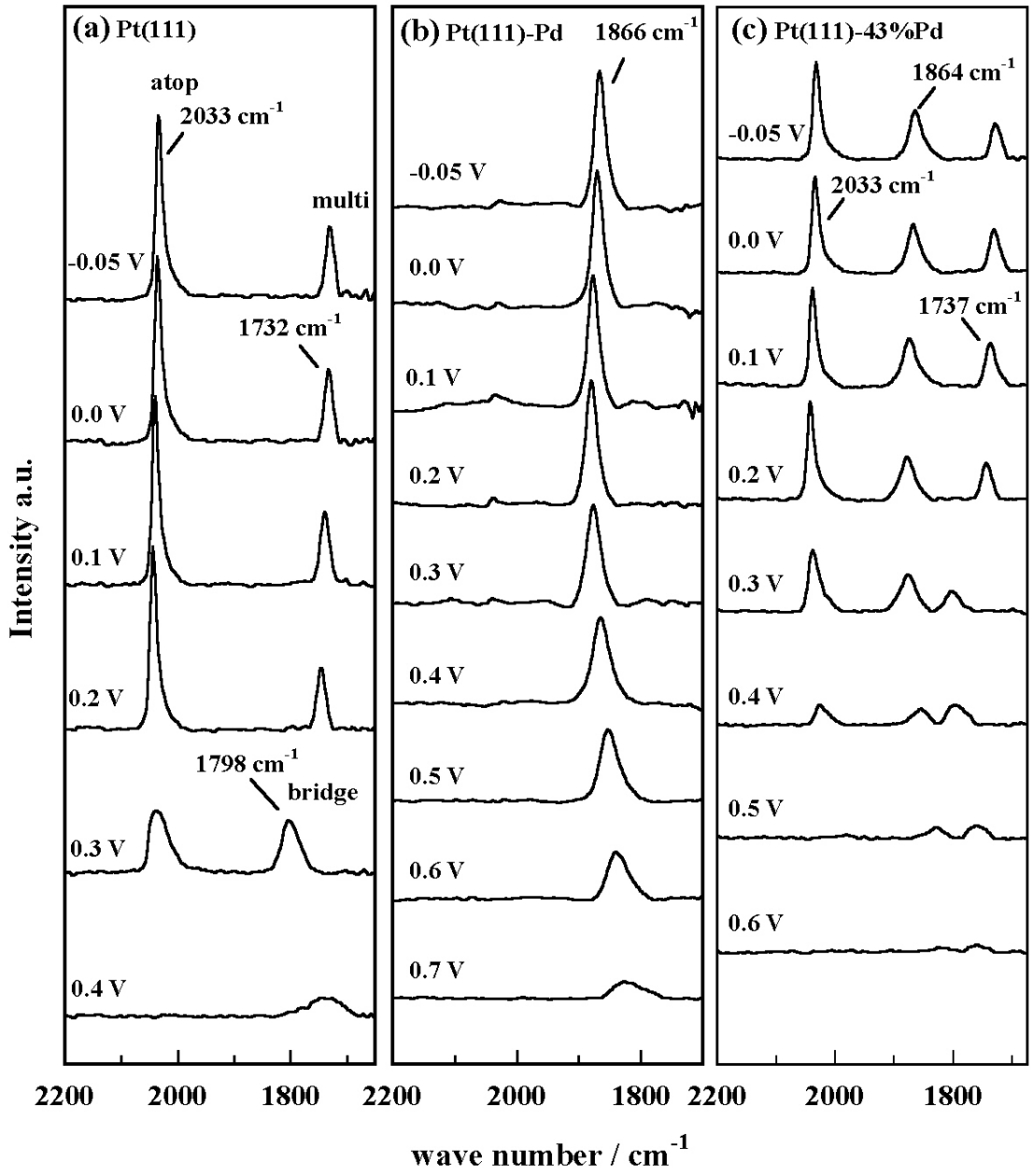

Arenz et al. figure 4

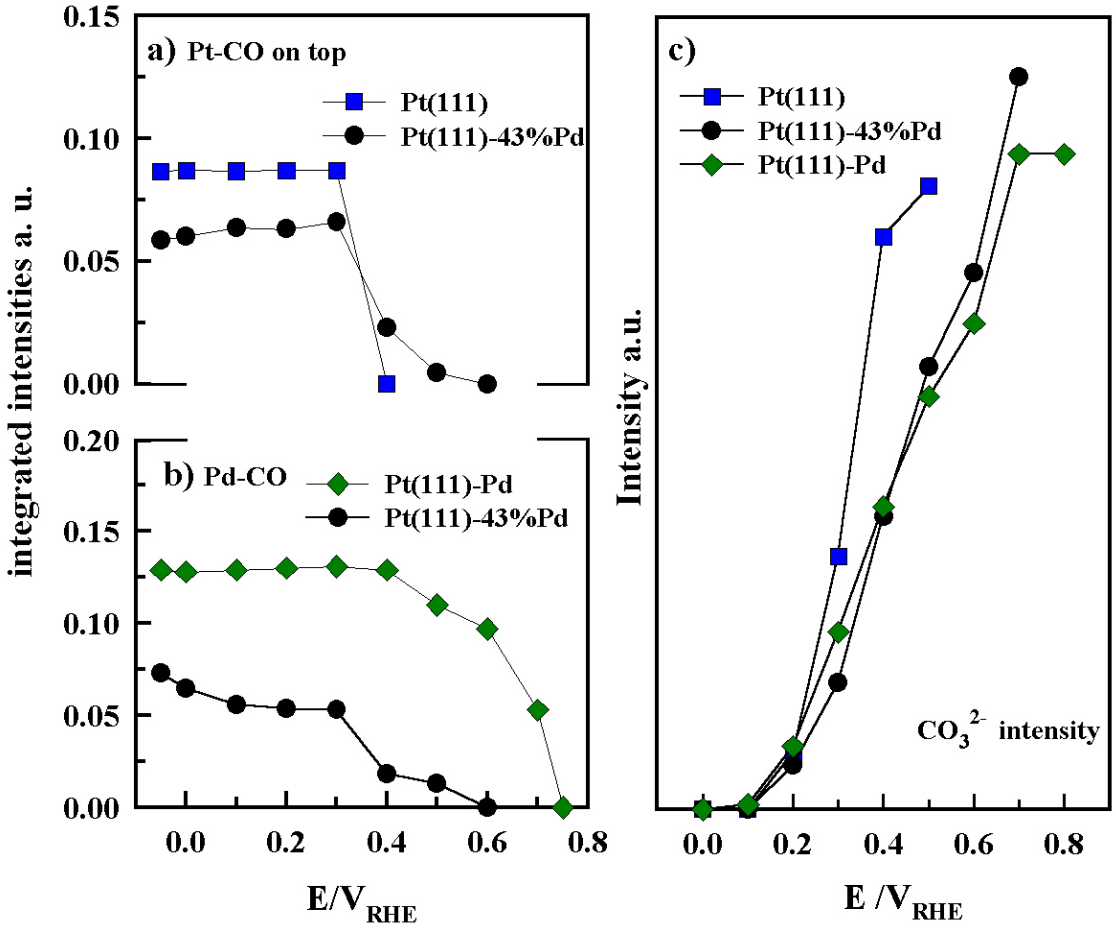

Arenz et al. figure 5